DOI: 10.13009/EUCASS2025-622
11TH EUROPEAN CONFERENCE FOR AERONAUTICS AND SPACE SCIENCES (EUCASS)

Towards Measurements of Non-Synoptic Atmospheric Boundary Layer Flows with an Instrumented Unmanned Aerial System

Peter Hartford[⋆ †], *Ewann Passelac Estrada* [⋆], *Balint Soós*[⋆], *Thomas Arnoult*[⋆], *Gertjan Glabeke*[⋆], *Julien Christophe*[⋆], *Félix Nieto* [□], *Hrvoje Kozmar*[◇], *Girma Bitsuamlak*[*], *Christophe Schram*[⋆]

[⋆]*von Karman Intitute for Fluid Dynamics, Waterloosesteenweg 72, 1640 Sint-Genesius-Rode, Belgium*
[□]*School of Civil Engineering, University of A Coruña, A Coruña, Spain*
[◇]*Faculty of Mechanical Engineering and Naval Architecture, University of Zagreb, Ivana Lučića 5, Zagreb, Croatia*
[*]*WindEEE, Western University, London, Canada*

[†]Corresponding author: peter.hartford@vki.ac.be

Abstract

An Unmanned Aerial System (drone) is equipped with an ultrasonic anemometer to obtain measurements of various wind profiles within a large scale wind tunnel facility (WindEEE). The drone system was traversed around 9 key measurement points within the wind tunnel in an attempt to obtain a spatial map of two different flow cases, including a horizontal Atmospheric Boundary Layer flow and a continuous vertical jet impinging on the floor of the wind tunnel. Considerations are put into the various problems that arise when using a drone, some of which require further mitigation in order to increase the reliability of the measurement system.

1. Introduction

Non-Synoptic Atmospheric Boundary Layer (ABL) flows, including downbursts and tornadoes, are a phenomenon that can cause huge amounts of damage to buildings and critical infrastructure (power lines and solar panels, for example). From 1980 to 2023, the European Union has suffered 214 Billion Euros worth of damages from storms, including high wind events, lightning, and hail.[1] As we continue to experience the effects of our changing climate, the frequency of these anomalous weather events will only increase, requiring further investigation into their underlying mechanics.

In addition to anomalous weather events, non-synoptic winds also appear in the wind energy sector, where both onshore and offshore wind farms can be subjected to unique flow regimes. Currently, there is a lack of predictive statistical models for these types of winds, requiring an exhaustive experimental database to fully characterize them.[12]

Non-synoptic flows are mainly characterized by their highly 3D and highly transient nature, often operating over short periods of time. The statistics of these flows will typically diverge from a Gaussian probability distribution, especially near the ground.[6] In addition to their non-gaussian nature, the vertical profiles will also diverge from a log-like profile that is typical of synoptic ABL flows, making modeling difficult.

Due to the relative infrequency and danger of these anomalous flows in nature, large-scale experimental facilities are required to accurately simulate these events. The WindEEE Dome facility is specifically designed to simulate these flows on a large scale, as its multi-fan design enables for a variety of different non-synoptic flows to be generated.[5] This is achieved with a large, individually controlled, fan array that can generate wind components in the vertical and horizontal direction. It provides ample opportunity to study and characterize these flows and gives a convenient test bed to develop new measurement systems that are suited for atmospheric flows.

Unmanned Aerial Systems (UAS), commonly referred to as drones, have shown particular advantages for the purpose of wind measurements. Anemometer-equipped drone systems have been frequently used for the purposes of atmospheric research, including atmospheric boundary layer studies, wind turbine wake analysis,[16] and particle concentration measurements.[9] For wind sensing, these systems typically operate using a few different sensing techniques, including 5-hole pressure sensors,[13] ultrasonic anemometers,[2,16] tethered Doppler LiDAR,[17] and even by using the motion of the drone itself.[7]

DOI: 10.13009/EUCASS2025-622

Despite the frequent use of drones in outdoor environments, drones could also be applied for use in large-scale facilities (like WindEEE). UAS systems have been tested in WindShape facilities,[11] providing valuable information about the reliability of drones under gusty atmospheric conditions. Considering the applicability of UAS systems in laboratory environments, there is clear potential for the use of drone-based anemometer systems to supplement or replace traditional traverse mechanisms for wind studies. One of the main advantages of a drone system is the ability for it to move around anywhere within the volume of interest, which can enable automatic measurements, and a potentially higher spatial resolution than traditional approaches.

This study presents one such system that was tested in the WindEEE facility under a variety of different conditions, including synoptic ABL flows and continuous vertical jet flows. A preliminary measurement database was generated and compared to a stationary ultrasonic anemometer fixed on the ground. The next section (2) presents the measurement platform, the experimental setup within the WindEEE facility, and the methods used to correct the anemometer measurements on the drone. Section 3 provides some preliminary measurement cases, and details where the drone can be advantageous compared to other measurement systems. Lastly, the conclusions and outlook are presented in Section 4 to provide an idea of where to go with the future of the drone-based anemometer system.

2. Methodology

The UAS platform flown in the WindEEE Dome facility is based on a Holybro X500v2 development kit, equipped with a TriSonica Ultrasonic Anemometer (USA).[8] A Raspberry Pi 5 (RPI5) companion computer was used to interface with the Pixhawk 6X flight controller and acquire the wind data from the USA. A recording is triggered when the user pulls a switch on the radio controller, passing the information from the flight controller to the companion computer (Figure 1).

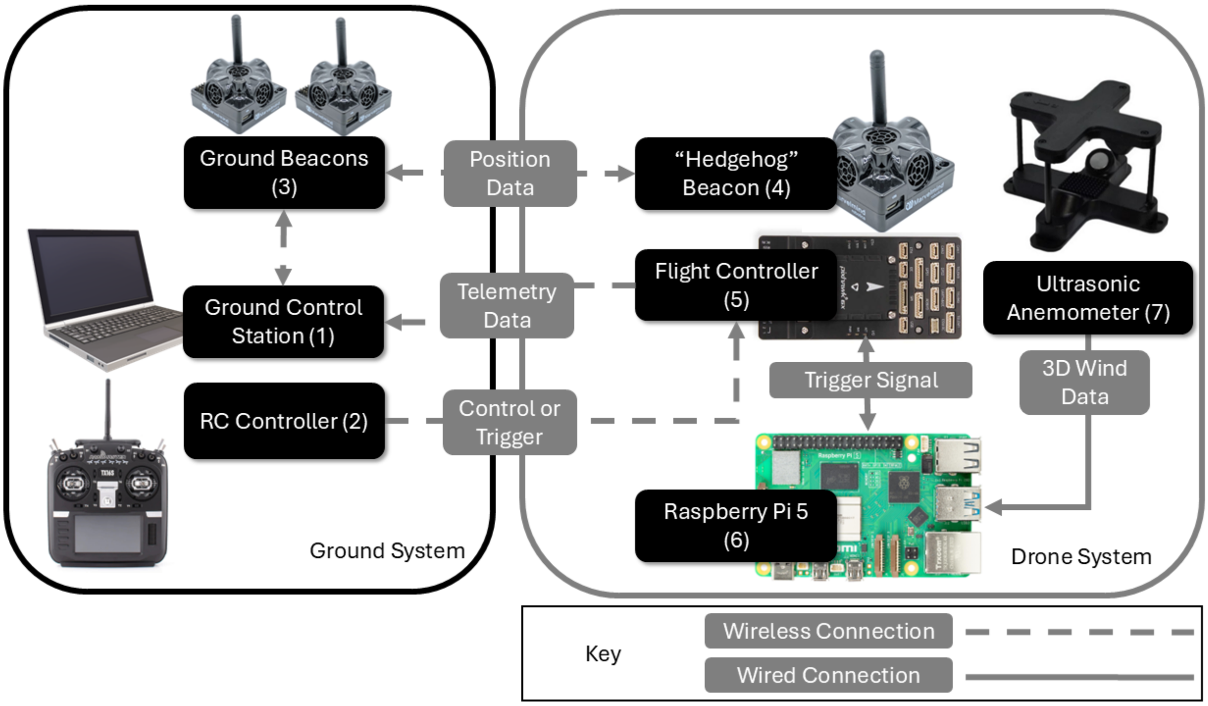

Figure 1: Overview of the ERIES drone system and its connections. 1. Ground Control Station, 2. RC Controller, 3. Ground Beacons, 4. "Hedgehog" Beacon, 5. Flight Controller, 6. Raspberry Pi 5, 7. Ultrasonic Anemometer. Wireless connections are indicated using a dashed line.

The drone position was estimated using a Marvelmind Ultrasonic Position System,[10] which operates using the travel time of ultrasonic waves between multiple stationary beacons, and a "hedgehog" beacon attached to the drone. This system has advantages in the ease of setup and lack of need for a calibration, but there can be issues when wind is present. The travel time of the ultrasonic waves will change based on the wind conditions, which can lead to higher uncertainties in the position estimation.

Additionally, the z-resolution of the system is highly dependent on the position of the stationary beacons, which can cause problems when the drone is operating in "position hold" mode, where the flight controller attempts to keep

DOI: 10.13009/EUCASS2025-622

the drone in the same position. Over the duration of this study, the drone was kept in "altitude hold" mode, requiring constant user control to maintain the drone's horizontal position. It should be noted that the Marvelmind was operating as a passive measurement device, without providing position data to the flight controller.

For each measurement, the drone was maneuvered to a target position, after which a short (15-60 second) acquisition of the ultrasonic anemometer was triggered. A Young 81000 Ultrasonic Anemometer[14] was placed downstream of the drone to provide a comparison of the wind measured by the drone. The position data from the Marvelmind system and the attitude of the drone was used to provide corrections on the velocity measured by the anemometer (Section 2.2).

It is important to understand the prevalent wind direction when conducting measurements with the TriSonica anemometer. From prior research,[4] it was found that the measurements are considered unreliable when the w-component of the wind vector (vertical direction) deviates by more than 15° from the horizontal plane (u-v plane). To address this issue when measuring the downward flow, the ultrasonic anemometer was fitted on a 90° elbow joint, enabling the u-v plane to be oriented vertically (Figure 2).

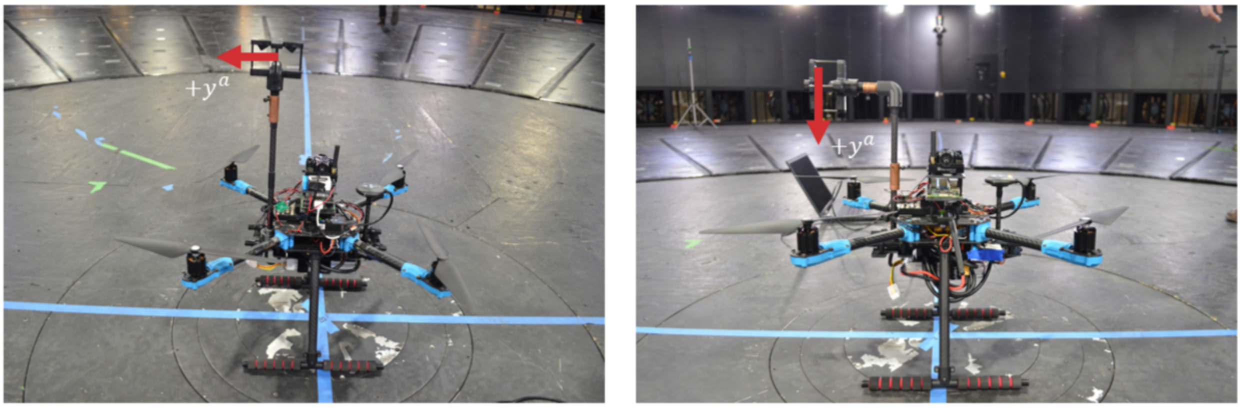

Figure 2: A Holybro X500v2 drone equipped with the TriSonica Ultrasonic Anemometer. Two configurations are shown, one with the u-v plane oriented horizontally (left) and one with the u-v plane oriented vertically (right). The red arrow indicates the direction of the anemometer's v-direction.

In a similar way to the directional limitations from the TriSonica system, the stationary anemometer system has problems when measuring flows with highly vertical components. The measurable range of the vertical component is ±60° (Table 1), which is problematic when measuring flows that dominate in that direction.

Table 1: Overview of available data and reliability from the stationary and drone-based ultrasonic anemometer systems.

	Drone System (TriSonica LI-550)[8]	**Stationary (Young 81000)[14]**
Sample Frequency [s^{-1}]	40	39.1
Measurable Speeds [ms^{-1}]	0 - 50	0 - 40
Wind Accuracy [ms^{-1}]	±0.2	±0.05
Horizontal Direction Accuracy [°]	±1	±0.1
Elevation Range [°]	±15	±60

2.1 WindEEE Experimental Campaign

As previously discussed, the WindEEE facility is designed for modeling non-synoptic wind profiles. The test chamber can be configured for a variety of purposes, with 100 individually controlled fans on the walls of the chamber, and 6 larger fans in the upper plenum.[6] For the purposes of this study, the test chamber was configured to produce a horizontal ABL and a continuous vertical impinging jet.

During the 2025 ERIES-SOLAR drone campaign (January 21^{st} to January 24^{th}), measurements were obtained of the aforementioned cases at varying fan speeds. A stationary ultrasonic anemometer (Young Model 81000) was used for comparison of the data from the drone system. Since the maneuverability of the drone remains difficult during extreme wind cases (intense downbursts and tornados), the test cases were limited to lower intensities.

DOI: 10.13009/EUCASS2025-622

The test matrix included measurements at 9 different locations with varying heights off of the ground (Figure 3b). For the horizontal ABL cases, the drone was flown at 1 and 2 meters from the ground. The vertical jet cases were obtained at positions closer to the ground (0.4 and 1 meter), due to the fact that the dynamics of these cases diverge from traditional analysis within the surface layer.[6]

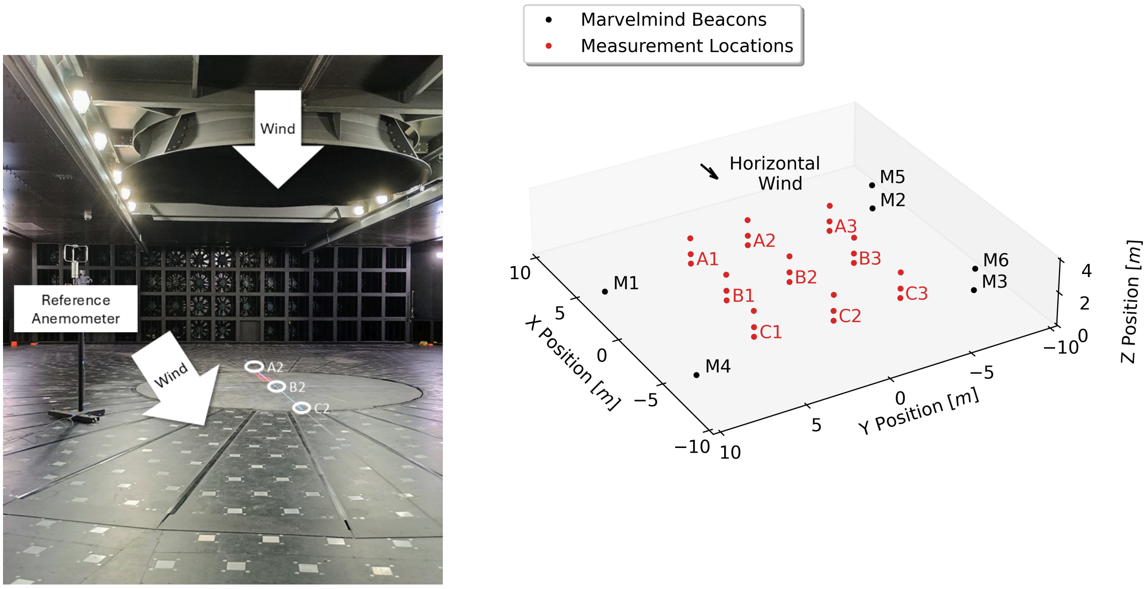

(a) The inside of the WindEEE facility with labeled measurement locations and wind directions.

(b) 3D Visualization of the targeted measurement locations, the horizontal wind direction, and the locations of the stationary Marvelmind beacons.

Figure 3: Experimental setup of the drone measurements inside of the WindEEE facility. A Young 81000 Ultrasonic Anemometer was used for comparison with the drone data.

2.2 Post Processing of Wind Data

There are a number of considerations that need to be accounted for in order to correct the data from the drone-mounted anemometer system. The wind data from the drone must be corrected for the motion of the drone (both orientation and velocity), the influence of the propeller system on the overall flow, and the interference between the ultrasonic positioning system and the ultrasonic anemometer. The full processing chain can be detailed in Equation 1, where the superscripts denote the reference frame of the vector component. The North-East-Down (NED) convention is used, with the "North" direction facing towards the horizontal fan array (Figure 4).

$$\begin{bmatrix} u^i \\ v^i \\ w^i \end{bmatrix} = \boldsymbol{R}^{id} \left(\boldsymbol{R}^{da} \begin{bmatrix} u^a \\ v^a \\ w^a \end{bmatrix} + \vec{I}^{d}_{prop} \right) + \begin{bmatrix} \dot{x}^i_{drone} \\ \dot{y}^i_{drone} \\ \dot{z}^i_{drone} \end{bmatrix} \tag{1}$$

2.2.1 Rotation of Wind Data to Inertial Frame

Two rotations need to be applied to transform the anemometer velocity into the inertial reference frame. A first rotation must be conducted to translate the raw anemometer velocity into the drone reference frame, which includes considerations for whether the anemometer is mounted in the "elbow" or "no elbow" configuration.

$$\boldsymbol{R}^{da} = \begin{cases} \begin{bmatrix} 0 & 0 & 1 \\ 1 & 0 & 0 \\ 0 & 1 & 0 \end{bmatrix}, & \text{elbow} \\ \begin{bmatrix} 0 & 1 & 0 \\ 1 & 0 & 0 \\ 0 & 0 & -1 \end{bmatrix}, & \text{no elbow} \end{cases} \tag{2}$$

DOI: 10.13009/EUCASS2025-622

The second rotation is based on the attitude from the drone, which is handled using a quaternion representation. This rotation matrix is a function of the measured attitude of the drone, and is thus dependent on the quality of the drone telemetry data. For this study, the drone attitude was sampled at approximately 1 Hz, reducing the reliability of the anemometer results at higher frequencies.

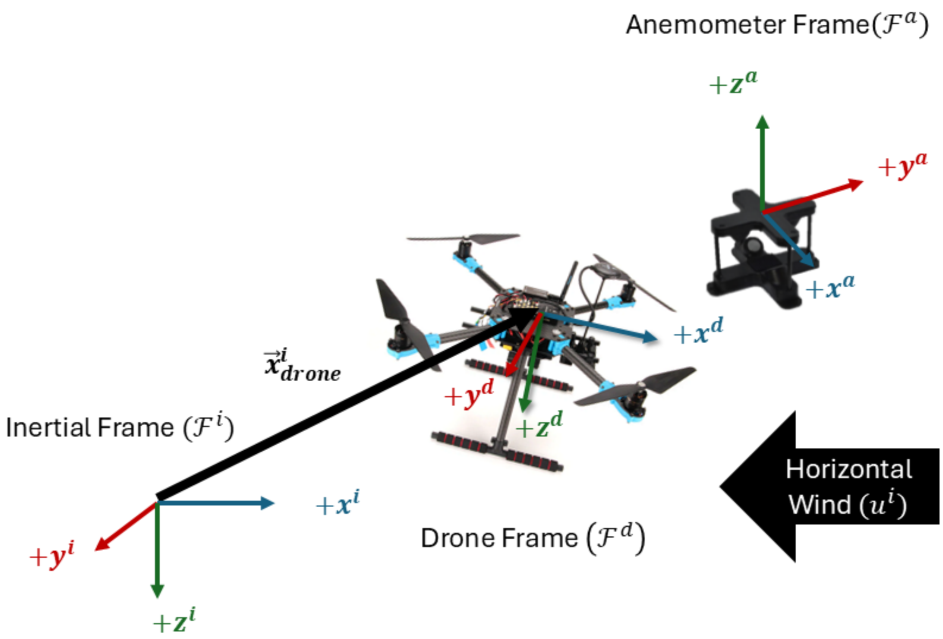

Figure 4: Schematic of the relevant reference frames, including the inertial, drone, and anemometer. The $+y^a$ direction points towards the anemometer's "north"

2.2.2 Interference from the Ultrasonic Position Sensor

It was found that the marvelmind beacons will create periodic spikes in the raw anemometer signal, which correspond to unrealistic velocities. This can heavily influence the statistics of the measurement if not dealt with properly. A two-step approach is taken to remove these fluctuations. The large peaks in the signal are first removed using a peak detection algorithm.[18] The moving statistics of the signal (mean (μ) and standard deviation (σ)) are then calculated and the peaks outside of $\mu \pm 2\sigma$ bounds are additionally removed.

2.2.3 Propeller Downwash Corrections

In addition to the corrections to the drone position and velocity, the vertical influence of the propeller system on the measurement must also be considered (Figure 5). In open air, the propellers typically do not have much of an influence on the horizontal wind measurements, but the vertical direction can prove to be quite troublesome.[16] Typical mitigation strategies for this issue come in the form of mounting the ultrasonic anemometer far away from the propellers, either by tethering it below the drone,[3] or by mounting it far away from the propellers ($\approx 5.3D_{prop}$).[19] For the purposes of wind tunnel anemometry these approaches can become cumbersome, due to the space constraints and stability requirements of the drone while in flight. In this study, the ultrasonic anemometer system was mounted at a height of 27 cm ($1D_{prop}$) from the propellers, which is well below the ideal value mentioned above.

Corrections on the vertical velocity component were thus considered using a simplified approach that was adapted from Thielieke,[16] which assumes that the propeller influence is uniquely vertical and only a function of the drone throttle (Equation 3), where A is an empirically determined factor. There are limitations to this approach, as the vertical influence is dependent on a wide number of factors, including individual propeller rotation rate (ω_{prop}), drone attitude ($\theta_{drone}, \phi_{drone}, \psi_{drone}$), drone altitude ($z^i_{drone}$), and sensor location ($\vec{x^d}_{sensor}$), as outlined in Figure 5.

$$\vec{I^d_{prop}} = \begin{bmatrix} 0 \\ 0 \\ At_{drone} \end{bmatrix} \tag{3}$$

DOI: 10.13009/EUCASS2025-622

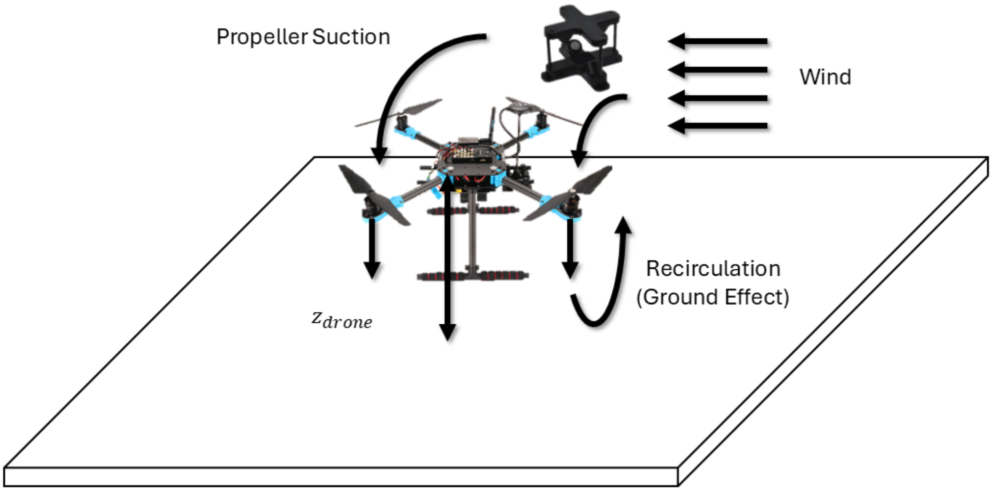

Figure 5: Sketch of the sources of influence from the drone propellers on the anemometer system.

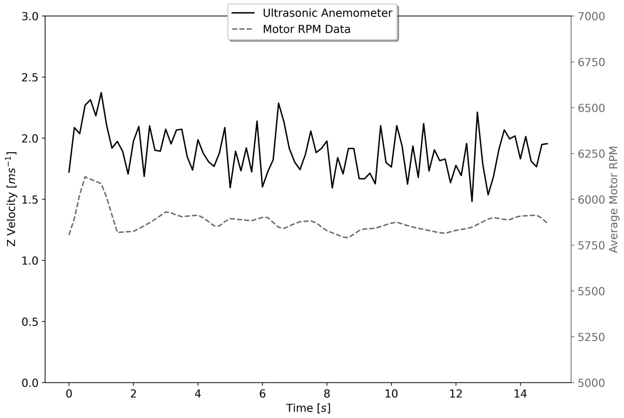

(a) Timeseries of the measured vertical velocity and the motor RPM data from the drone.

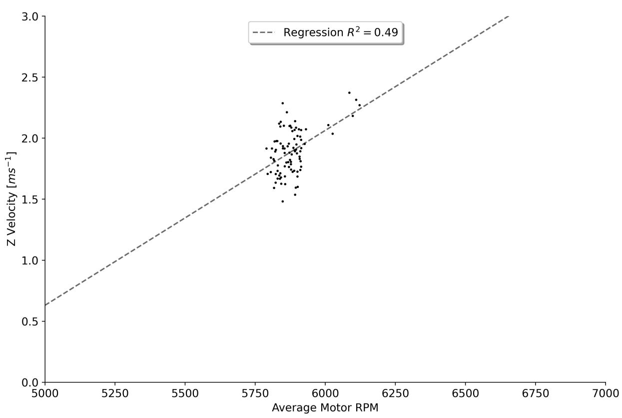

(b) Comparison of the of the measured vertical velocity and motor RPM data with a linear regression, $R^2 = 0.49$.

Figure 6: Investigation into the drone propeller influence on the ultrasonic anemometer data in the "elbow" configuration.

This approach was simplified even further to assume a constant correction factor, due to the poor regression of the relationship between motor RPM and vertical velocity from the campaign data (Figure 6b). An assumption like this can work because the drone throttle was relatively constant during the measurements. These corrections are only applied to the "elbow" cases, since it was found that the "no-elbow" cases don't see this influence as intensely due to the poor z resolution of the drone-mounted anemometer. When the drone is close to the ground, the recirculation of the propeller downwash will begin to induce a horizontal component on the anemometer, which can be another instance where this correction falls short (Figure 5).

$$\vec{I^d_{prop}} = \begin{bmatrix} 0 \\ 0 \\ -1.9 \end{bmatrix} \tag{4}$$

DOI: 10.13009/EUCASS2025-622

3. Results from the WindEEE Campaign

Two different flow cases are presented of the drone within the wind tunnel, showcasing the potential of the drone system to work as both a stationary and traversing sensor system. Stationary measurements were taken for the horizontal ABL flow to capture the statistics of the flow at different measurement locations. Traversing measurements were taken for the vertical jet case in an attempt to retrieve a horizontal profile of the jet at different intensities.

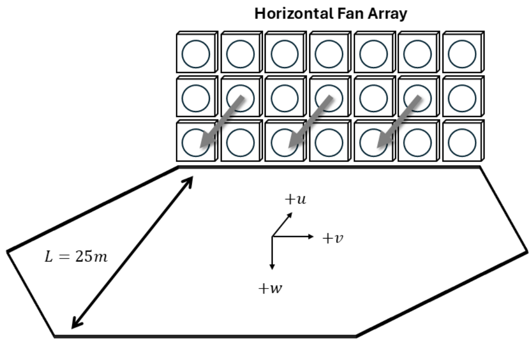

(a) Schematic of the horizontal ABL flow tests in the WindEEE facility. The horizontal fan array generated a continuous flow, and the drone was flown around the middle of the facility at $L/2$.

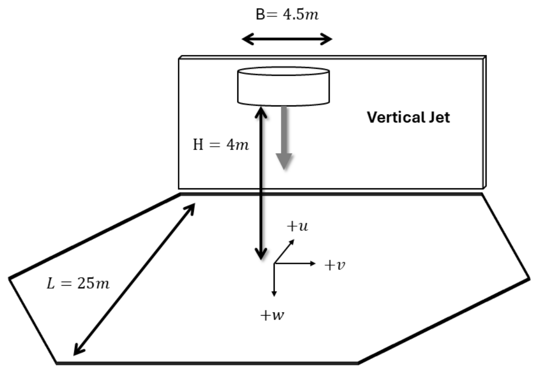

(b) Schematic of the vertical jet tests in the WindEEE facility. The vertical jet consists of a smaller fan array, that generated a continuous flow impinging on the floor of the wind tunnel.

Figure 7: Schematics of the two flow cases that are presented duing the WindEEE campaign.

3.1 Horizontal ABL Flow

The horizontal ABL flow cases were treated with special attention, to ensure that the measurements from the other cases are reasonable, and to give perspective on the problems that still need to be resolved. For the horizontal flow cases, the drone was flown at 2 meters above the ground ("B2" location), and stationary measurements were taken for 1 minute. These measurements were compared with the stationary anemometer downstream of the drone at the "C3" location (Figure 3b).

3.1.1 Spatial map at the measurement locations

A spatial map of the mean U component of the wind at 20% fan speed is shown (Figure 9) at the 9 different measurement locations for heights of 1 and 2 meters. The "B1" location observes the highest wind magnitude in comparison with the rest of the cases, which is not what would be expected. This can be due to aforementioned factors, including poor drone velocity estimation or propeller downwash. The other locations seem to respect the qualities that would be expected of horizontal ABL flow, including the fact that the average wind is higher when the drone measuring at a higher position.

3.1.2 Comparison of Different Fan Speeds

A visualization of the timeseries from the drone and stationary anemometer is shown in Figure 10 for different fan powers. A Reynolds decomposition was performed using the 1 second averaging window of the mean wind (Equation 5).

$$U(t) = U + u' \tag{5}$$

The horizontal turbulence intensity was estimated using the RMS of the fluctuations, as detailed Equation 6, where (U) is the mean horizontal velocity measured by the drone and u' is the fluctuating component. The mean horizontal component of velocity (U) is higher for the drone than the stationary anemometer, which can be attributed to the pressure loss of the wind tunnel.

$$T_u = \frac{\sqrt{\overline{u'^2}}}{U} \tag{6}$$

DOI: 10.13009/EUCASS2025-622

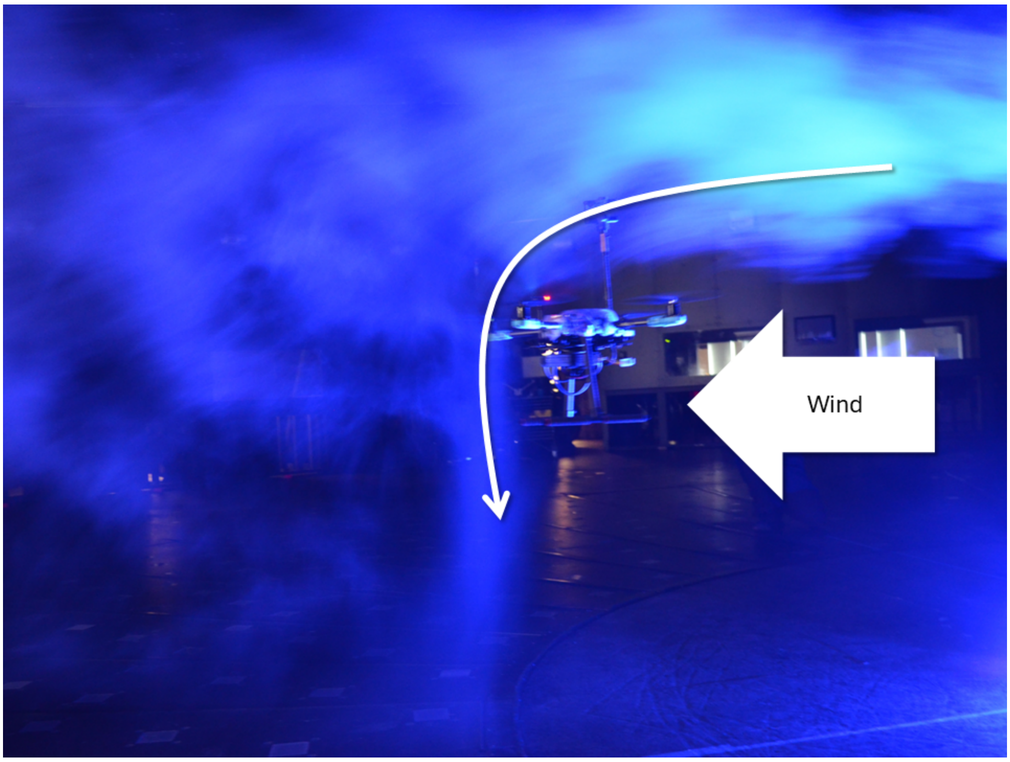

Figure 8: Flow visualization of the drone flying under horizontal ABL conditions, the prevalent wind direction is indicated with a white arrow. The additional arrow indicates the influence from the propeller system.

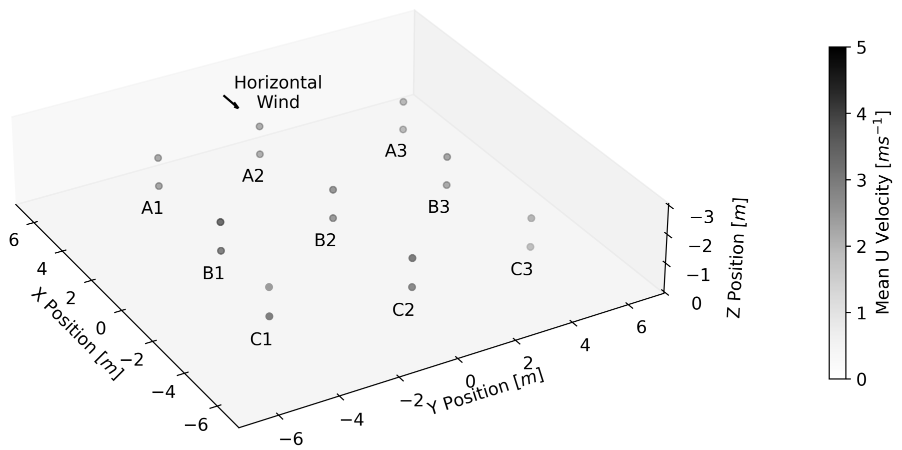

Figure 9: Spatial map of the mean wind measured by the drone at 20% fan speed.

DOI: 10.13009/EUCASS2025-622

The turbulence intensity is generally higher for the drone than the stationary anemometer (Table 2). This can be attributed to a few potential factors: the first being that the drone is upstream of the stationary anemometer, the second being that the drone propellers could be increasing the turbulence level, and finally because the drone-mounted ultrasonic anemometer might be better at capturing turbulent fluctuations than the stationary anemometer.

A second observation is that the stationary anemometer is reading a higher turbulence intensity at higher fan speeds, which is contrary to what should be the case. One reason for this could be that the drone propeller downwash will increase the turbulence level at higher wind speed, since the propellers have to spin faster to counteract the higher wind velocity.

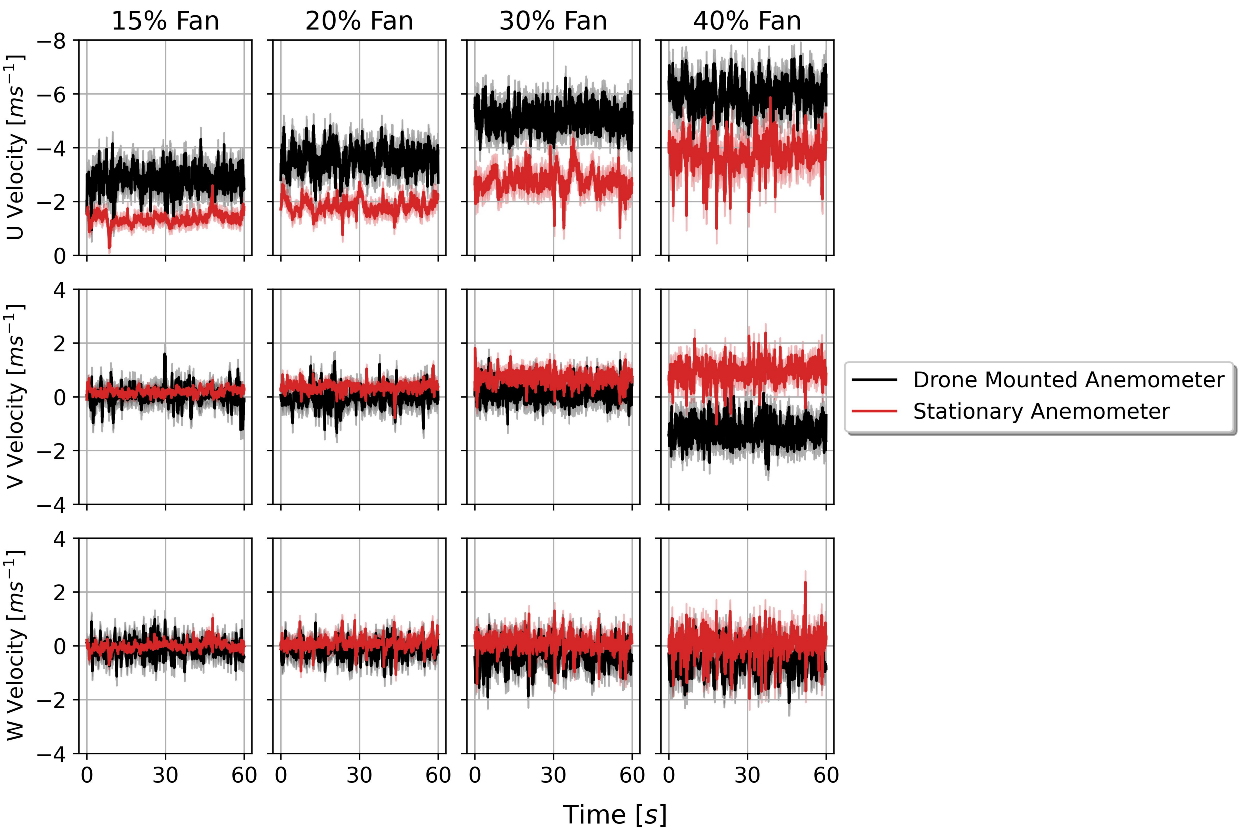

Figure 10: Sample timeseries comparison of the stationary anemometer and drone-mounted anemometer at two different locations with varying fan speeds. Error margins are indicated by the shaded regions.

Table 2: Horizontal components of mean and turbulence intensity for the 4 different horizontal ABL cases.

Case	**U (Drone) [ms^{-1}]**	**U (Stationary) [ms^{-1}]**	**T_u (Drone) [%]**	**T_u (Stationary) [%]**
Fan Speed: 15%	2.79 ± 0.44	1.36 ± 0.21	11.54	4.62
Fan Speed: 20%	3.54 ± 0.44	1.83 ± 0.26	8.83	4.23
Fan Speed: 30%	5.10 ± 0.43	2.75 ± 0.39	6.43	5.35
Fan Speed: 40%	5.78 ± 0.51	3.75 ± 0.56	6.24	7.64

3.2 Vertical Jet Flow

The WindEEE is typically able to generate a range of flows with a highly vertical component, including downbursts and vertical jets. For the purposes of this investigation, the downburst flow was deemed to be too strong for the drone to fly safely under those conditions. Thus, the experimental campaign focused on a steady vertical jet, with varying degrees of fan intensity.

For the vertical jet cases, profiles were acquired by traversing the drone horizontally through the measurement volume. In this case, the drone was traversed from the "C2" location to the "A2" location (figure 12a). Horizontal

DOI: 10.13009/EUCASS2025-622

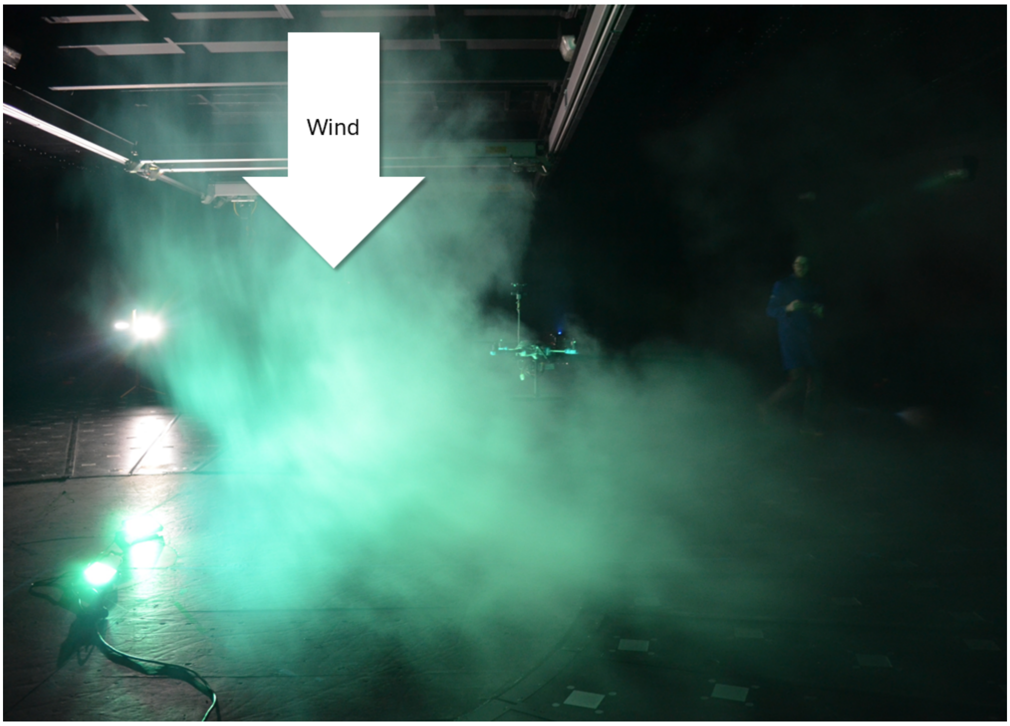

Figure 11: Flow visualization of the drone flying under downward flow conditions, the prevalent wind direction is indicated with a white arrow.

profiles were constructed of the vertical jet flow at 10% and 20% fan power by correlating the drone position data and the anemometer data. Spatial averaging was performed for one trajectory by creating a number of evenly spaced bins of 0.5 meters to construct a preliminary profile of the vertical velocity.

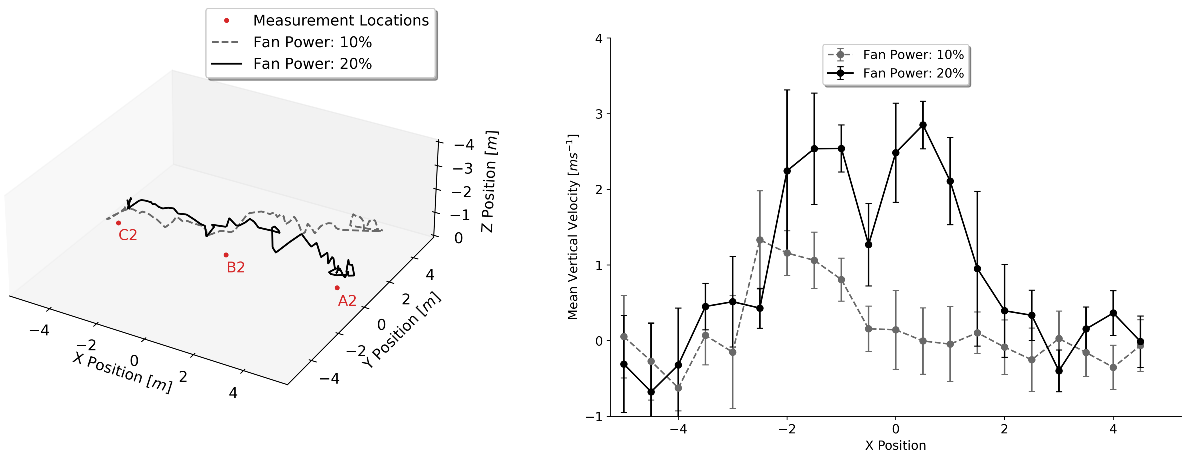

(a) Sample trajectories of the drone for the vertical jet cases.

(b) Averaged horizontal profiles of the vertical jet impinging on the floor of the WindEEE facility. These profiles were taken at a vertical distance of 3 meters from the jet opening. Results were spatially averaged with a bin size of 0.5 meters.

Figure 12: Results from the preliminary traverse cases of the drone flying through a jet vertical on the floor of the wind tunnel.

In Figure 12b, the profile at 20% fan speed has a higher magnitude of velocity than the one at 10% (which is to

DOI: 10.13009/EUCASS2025-622

be expected. The 20% case is relatively well constructed, showing a symmetrical profile with a stagnation region in the middle regions of the jet ($x = 0$). This is similar to what would be expected at this distance from the stagnation region.[15] The 10% case is of lower quality than the 20% case, which can be attributed to a multitude of factors, including low quality drone velocity estimation and deviation of the drone trajectory in the y-direction.

4. Conclusions and Outlook

In this paper, we present a novel drone-based anemometer system that is uniquely suited to probe a large scale facility, where traditional methods are too large or costly. A preliminary experimental campaign with this system was carried out in the WindEEE facility, showcasing the advantages and challenges of applying a drone for measurements within a wind tunnel.

Preliminary measurements of Atmospheric Boundary Layer and Vertical Impinging Jet flows were presented, showcasing the benefits and drawbacks of using a drone-based anemometer system. Corrections of the measurements are heavily dependent on the quality of the corrections for the added problems that come with using a drone system indoors. If the modeling of propeller downwash can be improved and the indoor localization is of higher quality, it is very possible to use this system reliably to reliably provide wind data indoors.

Future developments of the platform will be dedicated to the integration of a wider range of measurement systems, including hot wire anemometers and pressure sensors. Additional position estimation systems are currently being investigated to remove the problems with interference on the anemometer system and to improve the quality of the position estimate enough for automatic control routines. Implementation of a guided flying mode will enable higher positional accuracy and additional benefits, including tilt-based wind estimation and automatic measurements.

In addition to more sophisticated sensor technology and flight patterns, the measurement system would benefit greatly from implementing more sophisticated post-processing techniques. With access to higher resolution drone data, it would be possible to implement an combined state and wind estimation techniques (like an Extended Kalman Filter, for example). These improvements will also need to be supplemented by better corrections for the influence of the drone propellers on the wind measurement systems. Unfortunately, due to the available data from the campaign, this was not feasible.

Additional measurement campaigns can be carried out at WindEEE to maximize the benefits of the facility. Since the fans can be individually controlled, it is quite possible to simulate gusty environments for the purposes of conducting investigations into drone stability and control . Experiments on drone kinematics and wake characterization could be performed in a controlled, indoor environment, due to the large scale of the facility. The possibilities could be quite extensive with a drone-based measurement platform, as long as the measurement systems are small enough to fit on a drone.

In conclusion, drone-based anemometry systems have a high amount of potential to conduct measurements in large scale facilities, despite the numerous challenges with implementation. If the quality of the measurements can be improved, the drone system could be very beneficial towards enabling high frequency and spatially resolute measurements at a relatively low cost.

Acknowledgments

Our colleagues at the WindEEE have been very supportive of this work (Girma Bitsuamlak and Mark Jacob Parker) both during and after the experimental campaign. Additionally, we would like to extend gratitude to the von Karman Institute team who conducted the experiments at the WindEEE facility (Balint Soós, Thomas Arnoult, and Gertjan Glabeke).

This work is part of the transnational access project "ERIES-SOLAR", supported by the Engineering Research Infrastructures for European Synergies (ERIES) project (www.eries.eu), which has received funding from the European Union's Horizon Europe Framework Programme under Grant Agreement No. 101058684. This is ERIES publication number C90.

References

[1] Annual economic losses caused by weather - and climate - related extreme events in the EU Member States — eea.europa.eu. `https://www.eea.europa.eu/en/analysis/maps-and-charts/annual-economic-damage-caused-by-1?activeTab=8a280073-bf94-4717-b3e2-1374b57ca99d`. [Accessed 02-06-2025].

DOI: 10.13009/EUCASS2025-622

[2] Kevin A. Adkins, Christopher J. Swinford, Peter D. Wambolt, and Gordon Bease. Development of a sensor suite for atmospheric boundary layer measurement with a small multirotor unmanned aerial system. *International Journal of Aviation, Aeronautics, and Aerospace*, 7:1–14, 2020.

[3] M. Ghirardelli, S. T. Kral, E. Cheynet, and J. Reuder. Samurai-s: Sonic anemometer on a multi-rotor drone for atmospheric turbulence investigation in a sling load configuration. *Atmospheric Measurement Techniques*, 18(9):2103–2124, 2025.

[4] G. Glabeke, A. Gigon, T. De Mulder, and J. Van Beeck. How accurate are ultrasonic anemometers, calibrated in a laminar wind tunnel, under turbulent conditions? In *Journal of Physics: Conference Series*, volume 2767. Institute of Physics, 2024.

[5] Horia Hangan, Maryam Refan, Chowdhury Jubayer, Djordje Romanic, Dan Parvu, Julien LoTufo, and Adrian Costache. Novel techniques in wind engineering. *Journal of Wind Engineering and Industrial Aerodynamics*, 171:12–33, 12 2017.

[6] Horia Hangan, Djordje Romanic, and Chowdhury Jubayer. Three-dimensional, non-stationary and non-gaussian (3d-ns-ng) wind fields and their implications to wind-structure interaction problems. *Journal of Fluids and Structures*, 91, 11 2019.

[7] Gautier Hattenberger, Murat Bronz, and Jean Philippe Condomines. Estimating wind using a quadrotor. *International Journal of Micro Air Vehicles*, 14, 1 2022.

[8] LI-COR Environmental. *LI-550 TriSonica® MiniWind and Weather Sensor*, 2024. Available at `https://www.licor.com/support/LI-550/docs.html`.

[9] Zixia Liu, Martin Osborne, Karen Anderson, Jamie D. Shutler, Andy Wilson, Justin Langridge, Steve H.L. Yim, Hugh Coe, Suresh Babu, Sreedharan K. Satheesh, Paquita Zuidema, Tao Huang, Jack C.H. Cheng, and James Haywood. Characterizing the performance of a pops miniaturized optical particle counter when operated on a quadcopter drone. *Atmospheric Measurement Techniques*, 14:6101–6118, 9 2021.

[10] Marvelmind Robotics. *Marvelmind Indoor Navigation System Operating manual*, 2024. Available at `https://marvelmind.com/pics/marvelmind\_navigation\_system\_manual.pdf`.

[11] Flavio Noca, Guillaume Catry, Nicolas Bosson, Luca Bardazzi, Sergio Marquez, and Albéric Gros. Wind and weather facility for testing free-flying drones. In *AIAA Aviation 2019 Forum*. American Institute of Aeronautics and Astronautics, 6 2019.

[12] Fernando Porté-Agel, Majid Bastankhah, and Sina Shamsoddin. Wind-Turbine and Wind-Farm Flows: A Review. *Boundary-Layer Meteorology*, 174(1):1–59, January 2020.

[13] Joachim Reuder, Line Båserud, Stephan Kral, Valerie Kumer, Jan Willem Wagenaar, and Andreas Knauer. Proof of concept for wind turbine wake investigations with the rpas sumo. In *Energy Procedia*, volume 94, pages 452–461. Elsevier Ltd, 2016.

[14] R.M. Young Company. *Young Model 81000 Ultrasonic Anemometer*, 2008. Available at `https://www.youngusa.com/wp-content/uploads/2008/01/81000-9028I29.pdf`.

[15] Anuj Kumar Shukla and Anupam Dewan. Flow and thermal characteristics of jet impingement on a flat plate for small nozzle to plate spacing using les. *International Journal of Thermal Sciences*, 145:106005, 11 2019.

[16] William Thielicke, Waldemar Hübert, Ulrich Müller, Michael Eggert, and Paul Wilhelm. Towards accurate and practical drone-based wind measurements with an ultrasonic anemometer. *Atmospheric Measurement Techniques*, 14:1303–1318, 2 2021.

[17] N. Vasiljević, M. Harris, A. Tegtmeier Pedersen, G. Rolighed Thorsen, M. Pitter, J. Harris, K. Bajpai, and M. Courtney. Wind sensing with drone-mounted wind lidars: proof of concept. *Atmospheric Measurement Techniques*, 13(2):521–536, 2020.

[18] Pauli Virtanen, Ralf Gommers, Travis E. Oliphant, Matt Haberland, Tyler Reddy, David Cournapeau, Evgeni Burovski, Pearu Peterson, Warren Weckesser, Jonathan Bright, Stéfan J. van der Walt, Matthew Brett, Joshua Wilson, K. Jarrod Millman, Nikolay Mayorov, Andrew R. J. Nelson, Eric Jones, Robert Kern, Eric Larson, C J Carey, İlhan Polat, Yu Feng, Eric W. Moore, Jake VanderPlas, Denis Laxalde, Josef Perktold, Robert Cimrman,

DOI: 10.13009/EUCASS2025-622

Ian Henriksen, E. A. Quintero, Charles R. Harris, Anne M. Archibald, Antônio H. Ribeiro, Fabian Pedregosa, Paul van Mulbregt, and SciPy 1.0 Contributors. SciPy 1.0: Fundamental Algorithms for Scientific Computing in Python. *Nature Methods*, 17:261–272, 2020.

[19] Trevor C. Wilson, James Brenner, Zachary Morrison, Jamey D. Jacob, and Brian R. Elbing. Wind speed statistics from a small uas and its sensitivity to sensor location. *Atmosphere*, 13(3), 2022.